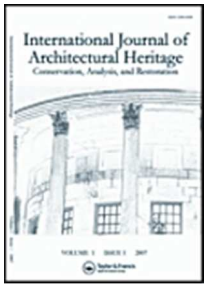

A collaborative engineering and archaeology project to investigate decay in historic rammed earth structures: the case of the medieval preceptory in Ambel

Journal:	*International Journal of Architectural Heritage*
Manuscript ID	UARC-2016-1475.R2
Manuscript Type:	Original Article
Date Submitted by the Author:	n/a
Complete List of Authors:	Miccoli, Lorenzo; Bundesanstalt für Materialforschung und –prüfung (BAM), Division Building Materials Gerrard, Christopher; Durham University, Department of Archaeology Perrone, Chiara; Ziegert | Roswag | Seiler Architekten Ingenieure Gardei, André; Bundesanstalt für Materialforschung und –prüfung (BAM), Division Building Materials Ziegert, Christof ; Ziegert | Roswag | Seiler Architekten Ingenieure
Keywords:	historical earthen building, rammed earth, materials characterisation, static monitoring, archaeology

A collaborative engineering and archaeology project to investigate decay in historic rammed earth structures: the case of the medieval preceptory in Ambel

Lorenzo Miccoli [a*], Christopher Gerrard [b], Chiara Perrone [c], André Gardei [a], Christof Ziegert [c]

[a] Bundesanstalt für Materialforschung und –prüfung (BAM), Division Building Materials, Unter den Eichen 87, 12205 Berlin, Germany

[b] Durham University, Department of Archaeology, South Road, Durham, DH1 3LE, United Kingdom

[c] ZRS Ziegert | Roswag | Seiler Architekten Ingenieure, Schlesische Straße 26, 10997 Berlin, Germany

[*]Corresponding author. Tel. +49 30 8104 3371 Fax +49 30 8104 1717 E-mail address: lorenzo.miccoli@bam.de

ABSTRACT

This study assesses the structural vulnerability of part of a later medieval earthen building at Ambel (near Zaragoza, Spain), once a preceptory or monastic house belonging to the Military Orders. An inspection of its morphology and materials coupled with the results of an extensive campaign of static monitoring reveals marked structural inhomogeneities, the product of more than a thousand years of construction, failure and repair from the 10th century to the present day. Building materials are inappropriately juxtaposed, there are discontinuities between construction phases and fundamental concerns remain over the long-term stability of the structure. The current condition of the structure is mainly influenced by structural discontinuities introduced at the time of construction, the unintended consequences of repair and modification and the material decay that has affected the base of the rammed earth walls. The overall findings of the static monitoring show that there is no related damage, variations in crack widths are related to the building seasonal cycle. While static analysis is an essential prerequisite before a suitable maintenance program can be fully defined, this study argues that no evaluation of the structural behaviour of any historic building can afford to ignore its archaeological 'biography' of modification and repair.

Keywords: historical earthen building, rammed earth, materials characterisation, static monitoring, archaeology

1 INTRODUCTION

Rammed earth is an earthen construction technique in which moistened earth is rammed in consecutive layers within a wooden formwork. In Spain, where this case study is located, rammed earth or *tapial* buildings are abundant and date from the Bronze Age onwards. The standing late 2nd century BC two-storied building at the centre of the acropolis at Botorrita, near Zaragoza, is a spectacular reminder of the durability of the technique (Beltran Martínez 1982). For some Islamic and later buildings, most famously the Alhambra in Granada, there is a long tradition of research by architects and art historians (eg. Torres Balbás 1981) and for some regions such as Granada (Martín Civantos 2009) and Seville (Graciani García 2009), precise typologies of materials are available. This goes some way to complementing a generation of significant archaeological results (eg. Gutiérrez Gonzalez 2002 for 11th–12th century urban Zaragoza; Tabales Rodríguez 2001) but while some rammed earth buildings do enjoy statutory protection (Jiménez Delgado and Cañas Guerrero 2006), their conservation and potential for restoration are less well studied (Jaquin and Augarde 2012; de la Torre López et al. 1991; Ontiveros Ortega 1995). The broader distribution and chronology of rammed earth structures remain uncertain, particularly so for later examples and more humble structures, while documentary evidence for materials, costs and labouring techniques has not yet been systematically collated across the Peninsula. Unless the circumstances were very exceptional, any proposal in which archaeologist, architect, engineer and historian are required to collaborate together to save a historic earthen building would be regarded as exotic at best. As a consequence, no matter how well meaning they may be, ill-advised restoration projects can attract hilarity and outrage in equal measure (The Guardian 2016).

The aim of this study is to investigate structural damage to a medieval building in Spain which is built in large part of earthen materials. We combine an investigation of the structure's overall decay in the light of a complex history with quantitative laboratory data, neither being without constraints of their own. A brief 'biography' of the building is presented first, together with details of its layout and construction materials. The second part of the study then explains the results of the campaigns of investigation both on- and off-site. The role and characteristics of the building materials are discussed, including their mechanical behaviour and decay parameters, together with an evaluation of the condition and evolution of the structure; methodological details have been reported upon previously (Miccoli et al. 2016). Several previous studies have underlined

the importance of understanding at least the most relevant cracks as part of the structural monitoring of any historical building (Carpinteri and Lacidogna 2006; Boscato et al. 2011; Lorenzoni et al. 2013) and that was a core aim here. The impact of changing temperature and humidity conditions are particularly highlighted below and, given that earthen structures are so sensitive to their environment, a programme of static monitoring of cracks was considered essential to assess ongoing trends in possible damage.

2 HISTORIC CHARACTERISATION, MORPHOLOGY AND MATERIALS

The building which forms the case study for this paper was intensively researched in the 1990s using a distinctively archaeological approach (Gerrard 1999; 2003). Existing plans of the building at 1:500 scale were enhanced, exterior façades were drawn at the same scale with interior sections at 1:20 and selected features measured at higher scales, and an exhaustive photographic record created. To this basic descriptive record were added distribution maps of material types (brick, stone rubble, rammed earth and adobe), which later proved fundamental to an understanding of the sequence of phases of construction and repair. Observations were also made of below-ground deposits whenever possible, during archaeological excavations, structural consolidation and the subsequent laying of services. Documentary research, in particular, proved to be essential when establishing the history of building, its phases of ownership and in some cases provided precise dates for visible repairs. In short, Ambel has become one of the best studied structures of its type and date in Europe and the original research archive has repeatedly informed decision-making during the conservation process. For the project described here the recording and interpretation of relevant areas of the structure was reviewed and revised, together with additional targeted archaeological excavation in two trenches to investigate the depth and nature of foundation levels both within the north-east tower and immediately to the west. This resulted in important changes to our understanding of the structural sequence in that part of the building, particularly the re-use of earlier architectural survivals as a basis for new construction and the definition of cycles of decay and damage.

During the Middle Ages and later, Ambel was a preceptory or commandery belonging at first to the Templars and later to the Hospitallers or Knights of Malta. In brief, over the centuries the role of the building was transformed from a fortified Islamic tower (ḥiṣn) into a monastic community and finally to a Renaissance palace. As is often the case for major medieval structures, there have been important

modifications and phases of demolition, particularly at the end of the 18th century and during the late 19th century when some upper storeys were removed altogether and the whole complex was re-roofed. These interventions give the complex its distinctive low silhouette today (Figure 1).

This study is confined to two parts of the complex. The first is a substantial rectangular tower (11 m × 7 m) on the southern side which is picked out in yellow on Figure 2b. The stone base of this south tower, 2.5 m in height, is currently judged to be 10th century in date on architectural and archaeological grounds and therefore pre-dates anything else on the site (Gerrard 2003). Its upper two storeys are rammed earth and wood recovered from its putlog holes has been radiocarbon dated to the 12th century, likely the date of a major phase of renovation around the time of the Christian conquest. Among its key architectural features are a first floor entrance and an arrow loop on its east side. This tower, with its many windows and doorways inserted at a later date, was probably maintained in use until the late 18th century: today it is a roofless shell.

The second part of the building under study here is the four-storey north-east granary tower (picked out in pink in Figure 2a-c) whose many phases of construction, collapse and repair can be documented from its elevations, architectural features, graffiti and historical records (Gerrard 2003; Jaquin 2008; Jaquin and Augarde 2004). Today, the leaning 15 m high north façade has become detached from the eastern and western walls; through-wall cracks up to 10 cm wide are clearly visible in Figure 3a,c and represent significant structural discontinuities which seem to affect the building's current stability. At the same time, the combination of stone and brick masonry with rammed earth creates changes in stiffness. In order to restore some structural continuity between the north façade and the adjacent walls perpendicular to it, a steel I-beam was introduced in 1998, followed by four more in the year 2000. These beams connect the façade to the underside of all the east-west timber beams spanning between the walls on three levels (all except the basement). The terminal H-plates on the north façade are clearly visible in Figure 3b.

Unlike its southern counterpart, the north-east tower is mostly built of monolithic rammed earth walls between masonry quoins, with the exception of the basement where stone and brick masonry predominate on the east and west sides, and on the north side where fired brick stands to a height of about 10 m. The first 3.2 m of this north façade consists of a pre-existing brick masonry garden wall dating back to the 14th century; the date of construction being indicated both by a decorative 'dog-tooth' brick frieze on its north façade and the relative sequence of building phases above. This garden wall is visible at the north end of the east façade

(Figure 4) where it turns to run N-S (Phase 2). It has no dug foundation, though there is archaeological evidence for an earlier precinct wall immediately adjacent (Phase 1). Between the 14th and 16th centuries other structures could be found here abutting the garden wall, the most obvious survivor today being the east wall of the north-east granary tower (Figure 4, Phase 3). This length of later medieval wall, which still stands to a height of 14 m and four storeys at its south end, is a survivor from an earlier granary on a similar footprint. At its south end it was once buttressed by a stair tower which provided exterior access from the east; a blocked doorway can still be seen in the attic (Figure 4).

During the mid-16th century there was a wider programme of investment at Ambel and by 1569, a date incised into the wet plaster of the granary columns at first floor level, the storage facilities in the north-east tower had been substantially expanded (Phase 4). Included in this refurbishment was a new north wall, a new west wall and the heightening of the east wall; anything solid that remained of earlier 14th–15th century structures was retained. The Phase 4 additions to the east façade are clearly seen on Figure 4 in the upper northern section of the elevation as well as on Figure 3a-c where the new 16th century lifts can clearly be picked out as a lighter shade of rammed earth, one lift having additional decorative brick. Reconstructing the final appearance of the tower, the current rectangular windows on the east façade (Figure 4, Figure 5) were probably once a short gallery of 16th century arches identical to those to be seen today on the north façade (Figure 1); this is suggested by the length of decorative bricks laid on end beneath. A matching length of bricks also now sits at the very top of the northern gable, and above these there would have been another gallery of round arched windows, a decorative brick eave and finally the roof (for a reconstruction see Gerrard 2003, Fig. 5.22). The height of the north-east tower at the end of the 16th century would therefore have been about 17.5 m with a rendered east façade rather than the weathered rammed earth we see today. The basement of this new tower was used as a wine cellar or *bodega*; in 1612, for example, 15 barrels are recorded as holding 23,760 litres (Gerrard 2003). According to graffiti preserved on their walls, the first and second floors held barley, wheat, oats and rye.

By the middle of the 18th century the structural condition of the tower had deteriorated considerably. The weight of cereals piled in the granaries exceeded the bearing capacity of their timber and plaster floors and this loading caused cracks to form in the eastern and western rammed earth walls due to the absence of a wall plate at ceiling height. The southern end of the second storey the floor eventually collapsed; damage can

be seen on the central supporting columns in the first floor granary (Figure 2b). To make repairs, replacement beams were then inserted through the middle of the eastern façade, the holes incised through the walls for this operation still being visible (Figure 3). Broken bricks were re-cycled to make good the granary floor. On another occasion, in 1739, money had been spent to repair the walls of the tower, very probably the filling of cracks and re-facing in brick at first and second floor levels in Figure 4 and Figure 5. Two decades later, in 1758, the stair-tower abutting the south-east corner of the north-east tower was demolished and the rectangular Phase 5 windows with their decorative brick eave inserted (Figure 3b and Figure 4). With entry from the east now sealed off entirely, new access arrangements to the tower had to be devised from the central courtyard by inserting internal stairs up through the floors.

Despite these bursts of investment, by 1795 the condition of the building had become so critical that partial demolition or abandonment were recommended to the commander of the building. In opting for the former, bold decisions were taken including the removal of the highest 16th century storey at the north end of the north-east tower, bringing the roofline down by 3 m. Structurally, this removed any substantial ties between the northern wall of the tower and the rest of the building. The minor brick ties shown on Figure 5 at attic level had probably already cracked through by this date and it was to compensate for this that timber elements were introduced at various points over the height of the façade (northern-to-eastern wall; northern-to-western wall) in order to re-connect the façade with the side walls. Only very minor repairs, however, were made after the building passed into private hands in 1851 (Phase 6).

In summary, the upper storeys of the south tower at Ambel are of 12th century date, while the north-east tower partially conserves at least three earlier phases of buildings ranging in date from the 12th to the 15th centuries (Phases 1–3) and what remains today is substantially of the mid-16th century (Phase 4). There is evidence for mismanagement of the granaries here which led to collapse of one of its floors and, once the building came to be rented out, so less attention was paid to the building's structural condition during the 18th century. Although major interventions succeeded in salvaging the more workable and profitable spaces (Phase 5), less thought was given to the future structural stability of the building and there were no major investments during the 19th century (Phase 6).

3 CAMPAIGNS OF INVESTIGATION

Three investigation campaigns were carried out between 2011 and 2012. These campaigns included a detailed survey which took the following morphological and structural characteristics into consideration:

- The presence of different materials with varying stiffness in the walls of the tower (rammed earth, rubble masonry, brick masonry). Construction phases are derived from Gerrard (1999, 2003).
- Variations in wall thickness together with the height of the structure and presence of openings.
- The existence of discontinuities such as through-wall cracks as shown in Figure 5.
- The structural system of horizontal elements, i.e. floors and roofs, with particular attention to their connection to the sidewalls. All floors in the north-east tower consist of timber joists spanned with narrow brick and plaster barrel vaults, while in the attic the ceiling is a simple system of primary and secondary beams. In the southern half of the basement, brick arches substitute for the timber beam structure found on all other floors.
- Stiffness discontinuities identified from visual surveys and the archaeological analysis of the preceptory´s construction history (e.g. the remains of a former precinct wall crossing the northern part of the granary tower, which creates differences in the relative stiffness of the wall bases) .

3.1 Materials characterisation

3.1.1 Sampling

In order to obtain information about material composition and mechanical data, samples of limited size were taken of the rammed earth (Figure 2a–c). Those materials with the earliest chronology, dating either side of the Christian conquest in the early 12th century, were removed in room 151 (R. 151) of the south tower. The rammed earth lifts here have corners of sand and lime (Gerrard 2003) but for the purposes of comparison the samples were taken from the lowest lift of rammed earth mid-way along the south wall, away from these areas of strengthening. A second set was extracted from the east wall of room 307 (R. 307) in the north-east tower; dating to the 12th or 13th centuries these construction materials certainly relate to the Templar phase of construction and occupation. Finally, samples from the eastern wall of room 302 (R. 302) at the site of the north-east tower were dated to the mid-16th century when the Hospitallers controlled the building. For moisture and salt analyses, samples were taken from R. 030, R. 139 and R. 301.

Before performing mechanical tests on earthen materials, conditioning was necessary because their strength is strongly dependant on moisture content (Miccoli et al. 2014; Jaquin et al. 2009). Storage of earthen materials samples at a constant RH until mass balance is reached is thus very important. In this study the recommended storage of samples at 23 °C and 50% RH (Röhlen and Ziegert 2010) adopted in German standards for earthen materials (DIN 18945 2013; DIN 18946 2013; DIN 18947 2013) was found to be suitable. The samples were transported in a closed waterproof container coated with a plastic foil to prevent them from dissolving in water (ASTM D7263 2009) and dried at 40 °C instead of 105 °C in order to avert the irreversible evaporation of any water trapped in the clay minerals.

3.1.2 Material composition

In this section an in-depth investigation of the physical, chemical and mineralogical properties with the aim to identify the composition of the building materials was carried out. On the base of these results the potential mechanisms of degradation were analysed, followed by the mechanical characterisation of the rammed earth. To obtain the composition of the binders in the earthen materials and their influence on the strength properties, particle size distribution (PSD) was determined according to DIN 18123 (1996) using sieve analysis. The PSD of local soil sample and the 12^{th}–13^{th} century sample from R. 307 are reported in Figure 6. In this case, it seems reasonable to assume that any difference in the particle size distribution can be attributed to natural variations in local sediment composition, though it is possible that some sand was deliberately introduced to reduce the clay content and so obtain an optimal mix. The 12^{th}–13^{th} century sample from R. 307 proved to be coarse-grained with a low fines (clay and silt) content ($d \leq 0.063$ mm) and a highly inhomogeneous PSD. What emerges from the results is that, while particle sizes < 10 mm in diameter show a good correlation with the envelope results devised by other researchers (Jaquin et al. 2009), a considerable portion of the mass of any given wall (approximately 30%) is not accounted for because it contains particles of diameter > 10 mm and up to 63 mm. As we shall see, the presence of these gravel-sized inclusions is not only interesting in terms of PSD.

Chemical and mineralogical analyses were then applied to identify the composition of the earth and clay minerals content X-ray powder diffraction (XRD) was used to characterise the phase composition of the earthen material samples and, in order to correlate the results with PSD, the XRD analysis was also

performed on a 12th–13th century sample from R. 307. Testing was focused on the finer components (d < 0.063 mm) and Figure 7 shows the phases detected in the material matrix. Quartz, calcite and feldspar are the main constituents of the grains. Illite, a non-swellable three-layer clay mineral, montmorillonite, a swellable three-layer clay mineral, and chlorite are the principal components of the clay fraction. Analysis of soils from the surrounding area (Figure 7) confirms that this soil also contains calcite and gypsum, albeit in much smaller quantities, but these results suggest that lime was not added.

Clay soil can be stabilized by the addition of small percentages, by weight, of lime (Bell 1996). However, a low percentage of burnt lime actually reduces the strength of the mixture due to the interactions between clay and lime (Minke 2001) and a high percentage is required to increase mechanical strength. When lime is added to the clay soil, it is first absorbed by clay minerals until the affinity of the soil for lime is achieved. This quantity, known as the 'lime fixation point', is normally in the range of 1–3% lime by weight of soil (Nagaraj et al. 2014), the exact percentage depending upon content and the kind of the clay minerals. Any additional lime will contribute to an increase in strength. In this case, although lime was used to reinforce the corners of the 12th century rammed earth lifts in R. 151 and in spite of the fact that burnt lime of suitable quality was locally available and already widely used - it is a primary material in Mudejar architecture in this part of Spain throughout the Middle Ages - the pure earth was judged to give sufficient mechanical strength for construction purposes and resistance to weathering. Comparison of XRD results from different rooms of the preceptory (Figure 8) and its various construction phases (R. 151, R. 302 and R. 307) confirm that the mineral phases of these three rammed earth samples are nearly identical and were therefore composed of the same raw material. The 16th century sample from R. 302 (Figure 2c) does contain more gypsum, however, indicating either a deliberate shift in composition or a change in sources of earth extraction. Visual analysis of the larger inclusions certainly suggests some chronological variation in composition, in particular residues from metal-working (slags), animal bone, pottery and tile were chosen as ingredients for later episodes of rammed earth construction in Ambel.

Micro X-ray fluorescence analysis (MXRF) in the form of elemental mapping of the sample extracted in R. 307 shows a large number of calcite grain components (Figure 9a), which correlates with the XRD results. The presence of calcium in the large aggregates (Figure 9b) indicates that calcitic pebbles were selected as a raw material for the rammed earth while the presence of sulphate phases as gypsum or anhydrite (Figure 9c)

implies that they are impurities from the source earth rather than being intentionally mixed in as a binder to improve and accelerate the construction process or increase structural stability. The migration of ions of sulphates by salt ingress can also be excluded as a possibility due to the location of the sample high on the wall (R. 307, internal) and, in any case, a finer distribution might be expected. It is also notable that silicon was dispersed throughout the binder matrix and detected in association with some aggregate grains (Figure 9d) and this confirms the presence of quartz particles suggested by the XRD analyses. Finally, sulphur was found in some of the aggregates where calcium was detected although it was not well distributed in the binder matrix. These aggregates are probably composed of gypsum. The addition of gypsum as a binder to accelerate the 'hardening process' of the rammed earth during wall construction seems unlikely because of its inhomogeneous distribution and, while gypsum is present in the grains, it is not found in the matrix. The results of this first part point out that the local soil was used to build the rammed earth walls without any changes in composition and any addition of lime or gypsum The lack of clay and silt fractions confirmed by PSD suggests a lower binder content with a negative effect on strength.

The identification of the mechanisms of degradation (for example the type of salt attack) is crucial, even more so when compatible repair materials must be developed. For this reason, cation and anion tests were carried out on samples collected at different heights along one axis of the eastern wall of the granary tower. The results in Table 1 confirm a high presence of chlorides and nitrates at the base, particularly at a height of 3–4 m above ground level, which corresponds to the base of the rammed earth wall overlying its stone rubble foundation. These high concentrations are a possible cause of the loss of cohesion of materials observed at this location. Given that the sample was taken from an upper level of the building (R. 301) it is unlikely to be affected by rising capillary action of soluble salts. The analysis of the reference sample proves that the raw materials of the rammed earth themselves do contain some salts.

The high proportion of Ca^{2+} and SO_4^{2-} at a height above 5 m is possibly linked to gypsum in the binder matrix or gypsum/anhydrite impurities in the earth at the time of construction. High percentage values of K^+, Na^+ and Cl^- meanwhile, while they can be associated with the presence of hygroscopic salts such as sodium and potassium chlorides, were mostly found in the basement and generally diminished with height. On this basis their presence might be due to capillary rise. For instance, some salts such as potassium sulphite might have leaked into the basement walls as a consequence of its use for wine-making and storage; alternatively,

the keeping of sheep in the building immediately adjacent on the east side of the granary tower may have led to elevated nitrate readings due to high concentrations of animal urine.

Chloride and nitrate levels are both quite elevated in all the samples taken, certainly with respect to values permitted for fired brick masonry (WTA 1999), and particularly so at lower levels where there is a maximum of 2.77 mass-% for nitrates and 0.63 mass-% for chlorides. Soluble salts have the same deleterious effects on earth as on other materials due to crystallisation pressure. Furthermore, hygroscopic salts increase the moisture content of the material as humidity rises. In this case the correspondence of humidity values and nitrate and chloride contents (Figure 10) confirms that the salts have been transported from beneath the ground through capillary rise.

The most visible and common consequence of high soil salinity and subsequent salt attack in earthen structures is an erosion pattern caused by the reduction of the wall cross-section; this is known as 'coving' (Fodde 2008). Normally, coving is attributed to soluble hygroscopic salts rising from the ground and, in the case of earthen buildings, attributed either to capillary rise or to the presence of salts in the soil used for the original construction of the rammed earth wall. The pressure deriving from the cyclic crystallization of salts destroys the structure of the building material from the surface inwards (evaporation threshold). Due to this loss of cohesion, affected walls have a cross-section which is effectively reduced by 5–10 cm from the original façade; this is in addition to any reduction caused by cross-sectional loss and does not take into account any further reduction in the compressive strength of the remaining section due to the capillary rise in moisture as well as an increase in moisture content caused by the increased salt content (hygroscopicity-induced) (Röhlen and Ziegert 2010). Whichever the cause, the overall effect is that the soluble salt content is directly proportional to both hygroscopicity and water absorption. Since the strength and the adhesive bond between soil particles are negatively affected when the base of the wall is saturated with water, the presence of salts is an indication of poor durability of the material. While coving in Ambel preceptory was found to be limited only, tests showed that highly soluble salts are nevertheless present, and our results indicate that these are hygroscopic in nature, particularly at basement level. Water content is relatively low at 2% here, but would register higher during wetter seasons, and the moisture content would account for a reduction in strength just as it has in previous studies (Miccoli et al. 2014).

To assess with greater accuracy the mechanical characterisation of the rammed earth, compressive strength, Young´s modulus and moisture content were all evaluated by testing samples removed from R. 307 (12th–13th centuries). Because of the slightly different gypsum content of this rammed earth confirmed by XRD analyses (Figure 8), test results provide only an approximate range of the tower's mechanical properties. Moisture content from on-site samples was found to range of 0.4–2.0% following a dry summer season in 2012. These values are relatively low and unlikely to bring about a significant decrease in compressive strength. However, the sample extracted on an upper storey at approximately 11 m (R. 307) in height showed a compressive strength of 0.75 MPa (Table 2).

To compare the results between samples of different sizes a reduction coefficient was adopted. Converted to a cubic sample 20 cm × 20 cm × 20 cm, which is the typical size of the samples tested for rammed earth, the compressive strength has to be reduced by a factor of 0.87 (ASTM C42 2013) with a final result of 0.67 MPa. The use of a coefficient of reduction is due to the different lateral confinement pressure applied on the cube during the test. This leads to the smaller cubes (10 cm × 10 cm × 10 cm) having a higher compressive strength than larger ones (20 cm × 20 cm × 20 cm). Once the samples were removed they were remixed after testing by forming regular cubes (10 cm × 10 cm × 10 cm) to eliminate negative influences on test results caused by sample extraction and irregular sample shape (Figure 11). This assumes that cohesion results mainly from clay minerals, which could be reactivated.

A comparison of mechanical properties (Figure 12) revealed that the remixed samples have more than 2.5 times higher compressive strength than the original samples extracted, and therefore within the range of minimum compressive strength required for load-bearing rammed earth (Volhard and Röhlen 2009). Young's modulus was also much higher for the remixed samples than for the original samples, even though the bulk density (DIN EN 1936 2007) of the original samples was similar. As no tests were carried out on the micro-structure of the materials, it is assumed that micro-cracks had occurred in the structure of the earthen material and that this explains the differences between original and remixed samples. Changes of temperature and humidity during the lifetime of the building or vibration during the various phases of extraction, transportation and sample preparation might all be responsible. Water content might also have played a key role. Summarising the mechanical properties of the rammed earth, the compressive strength of the rammed earth in the north-east tower might be slightly higher than the tested material from R. 307

because of its composition, namely the presence of additions or impurities in the soil, however the overall conclusion must be that the samples prepared from soil from the Ambel area performed well considering their lower bulk density.

3.2 Monitoring

Earthen structures are particularly sensitive to their environment and one of the aims of the research presented here was to monitor the impact of changing temperature and humidity conditions. Non-obtrusive static long-term monitoring was therefore set up in the north-east tower to record the movement of cracks and analyse their performance over the short-, medium-, and long-term. Short- and medium-term monitoring began in September 2011 while data from long-term monitoring are available since 1997. Two types of parameters (static and environmental) were recorded, interior and exterior temperatures with air humidity being taken every 30 minutes to assess the impact of thermal effects on the evolution of cracks. The layout of the sensors placement is shown in Figure 13, where letters S, M and L are related to the sensors used respectively for short-, medium- and long-term monitoring. Their placement is non-destructive and they are relatively unobtrusive.

Long-term monitoring, carried out by measuring variations in crack width at twelve different locations (L1–L12), had already identified an important displacement in the upper part of the north wall of the tower over the past 20 years, with separation cracks being visible today at the junction of the north wall with the east and west walls (Figure 3c). At the time the favoured diagnosis of this increase in crack width was the rotation of the upper façade on top of the ancient garden wall which at this location functions as a foundation (see above). The possibility of differential settlement in the foundation of the north wall was not considered likely and, in 2000, steel beams were introduced at all floor levels in order to improve connections with the lateral walls.

As part of the present study a more detailed inspection was undertaken around the east wall, here a major crack was found to run right through wall. For this reason, four linear differential variable transformers (LVDTs), indicated as S1–S4 shown in Figure 14a,b, were installed on the interior of the façade for a short-term monitoring. Other visible cracks on the east and west walls were monitored through medium-term

monitoring (M1–M7) using seven digital crack meters (Figure 14c). The thermo-hygrometer was placed close by near the central courtyard. Details on the location of sensors are provided in Table 3.

3.2.1 Short-term monitoring

Figure 15 shows variations in crack width over the course of three/four days in three different monitoring campaigns (Table 4), together with corresponding temperature changes and RH. For the first set of data (Figure 15a,d) there is no simple linear relationship between temperature and moisture changes, although there is an inverse proportionality between the two. Due to the high thermal inertia of rammed earth (Dong et al. 2014), there is a gap between the temperature variation and the crack width variation shown on the graphs. The LVDT measurements are coupled: S1–S2 belong to crack A and S3–S4 belong to crack B (Figure 14a). Consequently, their observed behaviour is similar, the upper sensors S3–S4 exhibit stronger levels of movement, possibly because the lower cracks are closer to the floor surface and therefore more constrained.

During August (Figure 15c,f) and September (Figure 15a,d) the greater opening of the cracks is largely related to diurnal temperature variation in the day-night cycle. At the end of August a temperature variation of 8.5℃ associated to a RH variation of 30.5% leads to a maximum variation in the crack width of 0.10 mm. As expected, during the measurements in November (Figure 15b,e) where the temperature variation in the day-night cycle is lower than in summer, the variation of the crack width is limited. A temperature variation of 3.8℃ associated to a RH variation of 20.0% leads to a maximum variation in crack width of 0.05 mm.

The effect of RH cannot be disassociated from the influence of temperature since their mutual variations are strictly connected.

On the upper set of graphs (Figure 15a–c), sensors S3–S4 behaviour are inversely related to internal temperature: as drying occurs and internal temperature decreases, so the crack width increases. This behaviour is expected; since each section of rammed earth should undergo linear shrinkage and decrease in length as temperature increases, so crack width must be expected to increase too. However, sensors S1–S2, which belong to the crack located between the fired brick and the rammed earth, exhibit a very different behaviour in which the width of the crack is directly proportional to the increase in temperature, that is to say, the crack width decreases slightly with a decrease in temperature. This is unexpected, but is best

explained by the effect of the rising external temperature on the steel beams connecting the outer façade to the inner floor beams. The effects of moisture on crack width are not directly noticeable in this case; they seem to be inversely proportional at one time and directly proportional to one another.

3.2.2 Medium-term monitoring

This system was set up over a period of 13 months, long enough to take into account the full annual thermal cycle. The sensors, based on a capacitive measuring system, were installed with a range of 25.4 mm, resolution of 0.01 mm and an accuracy of 0.02 mm. The results showed that the movement of the building to a large extent followed the temperature trend through the seasons – that is to say, there is a direct proportionality with temperature variation, with different coefficients. Comparison between displacement and temperature (Figure 16) paths clearly indicates the influence of thermal strain on the displacement values; generally the crack/interface opening increases during the five coldest months (October–February) but then begins to reduce over the next six months before again increasing. This reveals a noticeable influence of external temperature on the displacements which generally start decreasing from the month of March, and in all cases the graphs indicate that the initial increase in displacement appears to be recovered after the turnaround (Table 5).

In detail, sensors M2 and M4–M7 exhibit increasing displacement over time, by showing the progressive decrease in displacement with rising temperatures. The decrease in displacement after the turnaround is of the same order of magnitude as the previous increase (i.e. about -0.30 mm), indicating a progressive crack closure with an almost complete recovery. Sensors M2 and M7 record the highest differences in displacement, showing positive peaks of 0.26 mm (M2) and 0.65 mm (M7) during the warmest months (Figure 16c,d). In the case of sensor M2 (Figure 16c), the variation in peaks of crack width of 1 mm is related to a temperature variation of 24 °C. The cracks then close as the temperature falls and the width variation corresponds to the linear thermal expansion expected for a steel beam of length equal to 3 m. This behaviour would not be expected if it were not for the steel beams. On the other hand, sensors M1 and M3 controlling the most worrying crack at the corner with the north façade (Figure 16a) behave exactly as might be expected for earthen materials, by decreasing in width due to the expansion of sections as the temperature rises, and vice-versa. This might be due to a lower weight placed on the steel elements (here, only the weight

of roof, which is minor) which therefore do not influence movement in rammed earth. Another possibility is that the wall is damaged enough to consist of single sections. These sensors show limited displacements in the range of 0.08–0.12 mm over the whole monitoring period (Table 5).

3.2.3 Long-term monitoring

Long-term monitoring demonstrates that the upper façade-east wall crack has opened (Figure 17a), indicating rotation outwards, with the upper crack opening at a higher rate (and up to 5 mm over the space of 3 years) than the lower one until the steel elements were inserted after 2000. Up to this point in time, the northern-most crack on the second floor, measured with sensor L7, had also increased in width by a similar magnitude (5–7 mm) but, after the anchors were introduced, its width actually decreased by 4 mm. In the attic, the same crack measured with sensors L1 and L2, showed an increase in width with similar magnitude until 2000, then, after the anchors were introduced, although the cracks continued to widen, its increase ratio decreased significantly in comparison with the data measured before the intervention.

The adjacent crack on the east wall measured through the attic and the second floor with sensors L3, L4 and L8 (Figure 17b) is stable, no relevant increase in crack size were detected from the beginning of the monitoring. The behaviour of sensor L4, showing an unusual increase in crack size between 2002 and 2003, is due to an unexpected movement of one of the reference points and not related to any crack displacement. For this reason, the crack magnitude measured by sensors L4 must be considered the same as that shown by sensors L3 and L8. Sensor L5 (Figure 17c), controlling one of the largest cracks at the corner with the north façade presents a constant increase in width comparable with the values shown after 2001 by sensors L1 and L2. A similar trend, although with more limited magnitude, is shown by sensor L6 controlling a crack at a greater distance from corner with the north façade.

For the lower part of the building, no similar increase in crack size (Figure 17a,c) can be observed from the data available. Indeed, the crack measured by sensors L10–L12 (Figure 17d), although in proximity to the corner with the north façade, shows an increase in width constant but not comparable with the value reported by the upper cracks. This result strongly suggests that the rotation of the upper façade, possibly on top of the garden wall, might be another structural pathology in addition to non-uniform settlement of the tower.

Although the experimental results did not establish with certainty the causes of the cracks and deformation observed in the north-east granary tower, one favoured hypothesis is that there have been different settlements due to diverse foundation conditions, multiple construction phases, as well as singular and temporary influences, such as the overloading of the granaries which caused the floor to collapse. Because detailed information for the soil stratigraphy was absent in this case, the influence of soil layers on detected cracks and deformation cannot ultimately be assessed.

4 CONCLUSIONS

In conclusion, three points may be highlighted. First, while mechanical data on newly rammed earth materials are readily available, these can have limited applicability to historic buildings largely because of the variability of materials present on site and their differential weathering.

The correspondence between mechanical behaviour and the physical properties of this building material is strictly related to mineralogical and granulometric features. For this reason, physical, chemical and mineralogical analyses were applied to identify the composition of the earth and the mechanisms of degradation. The results pointed out that the local soil was used to build the rammed earth walls without any changes in composition and any addition of lime or gypsum. The PSD underlined a lower binder content with a negative effect on strength.

In the tests carried out for this research the historic earthen materials were considerably weaker than laboratory-tested new-build earthen materials. The latter should not be used as comparanda for the former. This may be due in part to their composition; in particular the soil is locally sourced and lacks finer particles, but may be attributed also to post-depositional impacts such as freeze-thaw cycles and other kinds of weathering such as water migration transporting fine clay particles. It is evident how far material decay can affect the base of rammed earth walls, especially where higher moisture and salt content levels are detected, and how these can negatively affect their compressive strength. Further studies are necessary on the direct correlation between salt, moisture contents and compressive strength; on freeze and thaw cycles on compressive strength; on thermal coefficients for these materials; on the effects of moisture on swelling and shrinking of rammed earth; on reasonable values for Young´s modulus in relation to moisture content and

also on how such Young´s moduli are to be calculated. The results reported here represent only the basic groundwork to understanding historical rammed earth structures, and in one case study alone.

Second, in seeking to explain the current condition of the medieval and later structure at Ambel, some factors such as structural discontinuities were introduced at the time of construction. More important however were the unintended consequences of repair and modification. These include weak or absent wall-to-wall connections, missing floor-to-wall connections and, in particular, the lack of wall plates to redistribute point loads. As confirmed in previous studies (Correia and Walliman 2014; Correia et al. 2015; Niroumand et al. 2016), in order to make sense of these observations the contribution of the buildings archaeologist is central and particularly so where structures have several phases of construction and demolition as they do here. In these cases it is the collaboration of engineers and archaeologists which provides the most secure platform for decision-making.

Third, the value of monitoring is paramount. The long-term crack monitoring carried out for the north-east tower after 1997 warned of progressive damage and led to the introduction of the steel anchors in 2000. More finely tuned short-term and medium term monitoring have the benefit of much higher accuracy and, as a result, the influence of climatic conditions on the building's behaviour during different seasons have been detected and quantified. The static monitoring activities described above were set up primarily to control the behaviour of the cracks on the external medieval façades of the building. The overall findings clarify the necessity of intervention at these locations and give clear indications about the static structural behaviour of the walls. On the basis of the results above discussed it is reasonable to assume that the east, the west and the north façades of the north-east tower are stable – variations in crack widths here are physiological and related to the normal seasonal cycle of the building; there is no related damage.

With the results data to hand it should now be possible to establish a plan of conservation for the building, possibly by improving further its box-type behaviour by securing wall-to-wall connections and floor stiffening, but also by replacing damaged rammed earth when the size of the crack width does not permit grouting (Silva et al. 2016; Müller et al. 2016). Nowadays, different solutions are available for historic rammed earth structures (Silva et al. 2014; Mileto et al. 2012; Canivell et al. 2012). However, the reintegration of missing sections of rammed earth walling is not so easily achieved (Vegas et al 2014), not only because the original rammed earth mix may consist of (by modern standards) poor materials or

inaccessible ones, but also because the relatively small proportion of binder present in the composition acquires its strength not from the properties of the materials themselves, but from a building technique which is based on vertical compaction. In addition, the high shrinkage rates of rammed earth (up to 2%) present some drawbacks to durability though this might be overcome by a programme of filling and replacement using high quality earth block masonry and plastering (Bardel and Maillard 2002) which should provide a compressive strength comparable to the surrounding rammed earth. The improvement of the box-type behaviour and the replacement of the damaged rammed earth areas would be both an effective way to reduce the structural vulnerability of the preceptory at Ambel and secure its life for the future.

ACKNOWLEDGEMENTS

This research was developed within the framework of NIKER (new integrated knowledge-based approaches to the protection of cultural heritage from earthquake-induced risk), a FP7 research project funded by the European Commission under contract No. 244123 to develop and validate innovative materials and technologies for the systemic improvement of the seismic behaviour of cultural heritage assets (www.niker.eu). The authors wish to acknowledge Ms. Caroline Kaiser, Dr. Christian Lehmann and Ms. Elgin Rother for their important support in material analyses and elaboration of results and Dr. Patrick Fontana and Mr. Nick Watson for their support during our investigation campaigns.

REFERENCES

ASTM C42. 2013. Standard test method for obtaining and testing drilled cores and sawed beams of concrete. American Society of Testing and Materials.

ASTM D7263. 2009. Laboratory determination of density (unit weight) of soil specimens. American Society of Testing and Materials.

Bell, F. G. 1996. Lime stabilization of clay minerals and soils. *Engineering geology* 42:223–237.

Beltrán Martinez, A. 1982. Archaeological excavations at Contrebia Belaisca (Botorrita, Zaragoza), 1980 (Excavaciones arqueológicas en Contrebia Belaisca (Botorrita, Zaragoza), 1980). *Noticiario Arqueológico Hispánico* 14:319–364.

Boscato, G., S. Russo and F. Sciarretta. 2011. Structural monitoring of the slender double-layered façade of Palazzo Ducale in Venice - Preliminary analysis of measurements. *Masonry International* 24:57–72.

Canivell, J., and A. Graciani García. 2012. Critical analysis of interventions in historical rammed-earth walls–military buildings in the ancient Kingdom of Seville. In C. Mileto, F. Vegas and V. Cristini (eds) *Rammed Earth Conservation*. Leiden, The Netherlands: CRC Press/Balkema, 289–295.

Carpinteri, A., and G. Lacidogna. 2006. Structural monitoring and integrity assessment of medieval towers. *Journal of Structural Engineering* 132:1681–1690.

Correia, M., L. Guerrero, and A. Crosby. 2015. Technical strategies for conservation of earthen archaeological architecture. *Conservation and Management of Archaeological Sites* 17:224–256.

Correia, M., and N. S. R. Walliman. 2014. Defining criteria for intervention in earthen-built heritage conservation. *International Journal of Architectural Heritage* 8:581–601.

de la Torre López, M. J., J. Rodríguez Gordillo, and E. Sebastián Pardo. 1991. Presence of Nazari gypsum mortars and concretes in the Alhambra (Presencia de yeso en morteros y hormigones Nazaríes en la Alhambra). *Boletín de la Sociedad Española de Mineralogía* 14:3–4.

DIN 18123. 1996. Soil, investigation and testing- Determination of grain-size distribution. Beuth Verlag.

DIN 18945. 2013. Earth blocks – Terms and definitions, requirements, test methods. Beuth Verlag.

DIN 18946. 2013. Earth masonry mortar – Terms and definitions, requirements, test methods. Beuth Verlag.

DIN 18947. 2013. Earth plasters – Terms and definitions, requirements, test methods. Beuth Verlag.

DIN EN 1936. 2007. Natural stone test methods – Determination of real density and apparent density, and of total and open porosity. Beuth Verlag.

Dong, X., V. Soebarto, and M. Griffith. 2014. Strategies for reducing heating and cooling loads of uninsulated rammed earth wall houses. *Energy and Buildings* 77:323–331.

Fodde, E. 2008. Structural faults in earthen archaeological sites in central Asia: analysis and repair methods. In *Proceedings of 6th International Conference on Structural Analysis of Historical Constructions*. Bath, United Kingdom: Taylor & Francis, 1415–1422.

Gerrard, C. 1999. Opposing identity: Muslims, Christians and the Military Orders in Rural Aragon. *Medieval Archaeology* XLIII:143–160.

Gerrard, C. 2003. *Landscape and lordship: the parish house of Ambel (Zaragoza). Archeology, architecture and history of the religious orders of the Temple and the Hospital (Paisaje y señorío: la casa conventual de Ambel (Zaragoza). Arqueología, arquitectura e historia de las órdenes religiosas del Temple y del Hospital).* Zaragoza, Spain: Institución Fernando el Católico.

Graciani García, A. 2009. The technique of rammed earth in western Andalusia (La técnica del tapial en Andalucía occidental). In A. Suárez Márquez (ed) *Construir en al-Andalus. Monografías del Conjunto Monumental de la Alcazaba*: Sevilla, Spain: Consejería de Cultura de la Junta de Andalucía, 111–140.

Gutiérrez Gonzalez, F. J. 2002. *La excavacion arqueologica del paseo de la Independencia de Zaragoza (The archaeological excavation of Paseo de la Independencia at Zaragoza)*. Zaragoza, Spain: GrupoEntorno.

Jaquin, P., and C. Augarde. 2012. *Earth building. History, science and conservation*. Garston, United Kingdom: IHS BRE press.

Jaquin, P. 2008. Study of historic rammed earth structures in Spain and India. *The Structural Engineer 86*:26–32.

Jaquin, P. A., C. E. Augarde, and C. Gerrard, 2004. Analysis of Tapial structures for modern use and conservation. In *Proceedings of 4th International Conference on Structural Analysis of Historical Constructions*. Padua, Italy: A.A. Balkema Publishers:1315–1321.

Jaquin, P. A., C. E. Augarde, D. Gallipoli, and D. Toll. 2009. The strength of unstabilised rammed earth materials. *Géotechnique* 59:487–490.

Jiménez Delgado, M. C., and I. Cañas Guerrero. 2006. Earth building in Spain. *Construction and Building Materials* 20:679–690.

Lorenzoni, F., F. Casarin, C. Modena, M. Caldon, K. Islami, K., and F. da Porto. 2013. Structural health monitoring of the Roman Arena of Verona, Italy. *Journal of Civil Structural Health Monitoring* 3:227–246.

Martín Civantos, J. M. 2009. Systemisation and dating of the Andalusians construction techniques in the territory of Ilbira-Granade: the case of rammed earth made of lime and gravels (Sistematización y datación de las técnicas constructivas Andalusíes en el territorio de Ilbira-Granade: el caso del tapial de cal y cantos). In Á. Suárez Márquez (ed) *Construir en Al-Andalus. Monografías del Conjunto Monumental de la Alcazaba*: Sevilla, Spain: Consejería de Cultura de la Junta de Andalucía, 205–232.

Miccoli, L., U. Müller, and P. Fontana. 2014. Mechanical behaviour of earthen materials: a comparison between earth block masonry, rammed earth and cob. *Construction and Building Materials* 61:327–339.

Miccoli, L., C. Perrone, A. Gardei, C. Ziegert, C. Kaiser, P. Fontana, and C. Gerrard. 2016. Analysis and diagnosis of earthen buildings: the case of Ambel preceptory in Aragon, Spain. In H. Feiglstorfer (ed) *Earth constructions and tradition*. IVA-ICRA, Vienna:203–231.

Mileto, C., F. V. López-Manzanares, V. Cristini, and L. G. Soriano. 2012. Restoration of rammed earth architecture in the Iberian Peninsula: Ongoing research. In C. Mileto, F. Vegas and V. Cristini (eds) *Rammed Earth Conservation*. Leiden, The Netherlands: CRC Press/Balkema, 381–386.

Müller, U., L. Miccoli, and P. Fontana. 2016. Development of a lime based grout for cracks repair in earthen constructions. *Construction and Building Materials* 110:323–332.

Minke, G. 2001. *The new earth building manual: building materials, constructions, earth architecture (Das neue Lehmbau-Handbuch. Baustoffkunde, Konstruktionen, Lehmarchitektur)*. Staufen im Breisgau, Germany: Ökobuch.

Nagaraj, H. B., M. V. Sravan, T. G., Arun, and K. S. Jagadish. 2014. Role of lime with cement in long-term strength of Compressed Stabilized Earth Blocks. *International Journal of Sustainable Built Environment* 3:54–61.

Niroumand, H., J. A. Barcelo, and M. Saaly. 2016. The role of archeology on earth buildings and earth architecture in the world. *Indian Journal of Science and Technology* 25:1–7.

Ontiveros Ortega, E. 1995. *Study of the materials used in the construction of the rammed earth at the Granada city walls (Estudio de los materiales empleados en la construcción de los tapiales de las Murallas de Granada)*. Unpublished PhD thesis. Granada University, Spain.

Röhlen, U, and C. Ziegert 2011. *Earth building practice: planning, design, building*. Berlin, Germany: Bauwerk.

Silva, R. A., P. Jaquin, D. V. Oliveira, T. F. Miranda, L. Schueremans, and N. Cristelo. 2014. Conservation and new construction solutions in rammed earth. In A. Costa, J. Miranda Guedes and H. Varum (eds) *Structural rehabilitation of old buildings*. Berlin Heidelberg, Germany: Springer, 77–108.

Silva, R. A., D. V. Oliveira, L. Schueremans, T. Miranda, and J. Machado. 2016. Effectiveness of the repair of unstabilised rammed earth with injection of mud grouts. *Construction and Building Materials* 127:861–871.

Tabales Rodríguez, M. Á. 2001. Contributions of archeology to the knowledge of medieval building techniques (Aportaciones de la arqueología medieval al conocmiento de las técnicas constructivas). in A. Graciani Garcí (ed) *La técnica de la arquitectura medieval*. Sevilla, Spain: University of Sevilla, 35–74.

The Guardian. 2016, 'What the hell have they done?' Spanish castle restoration mocked. http://www.theguardian.com/world/2016/mar/09/matrera-castle-cadiz-spain-restoration-mocked, accessed March 2016.

Torres Balbás, L. 1981. Dispersed work: archaeological chronicle of Muslim Spain (Obra dispersa: crónica arqueológica de la España Musulmana). *Crónica* 45:205–207.

Vegas, F., C. Mileto, and V. Cristini. 2014. Constructive features and preservation work of rammed earth architecture: the Islamic tower of Bofilla (Valencia). *Journal of Architectural Conservation* 20:28–42.

Volhard, F., and U. Röhlen. 2009. *Earthen construction rules: terms – building materials –components (Lehmbau Regeln: Begriffe – Baustoffe – Bauteile)*. Wiesbaden, Germany: Dachverband Lehm e.V. Vieweg + Teubner Verlag.

WTA Technisches Merkblatt. 1999. Assesment of masonry – masonry diagnostic (Beurteilung von Mauerwerk –Mauerwerksdiagnostik). *Merkblatt 4–5–99/D*. Munich, Germany: WTA Publications.

LIST OF FIGURES CAPTIONS

Figure 1. Ambel preceptory.

Figure 2. Ambel preceptory. Location of rammed earth samples: (a) ground floor plan with sampling location from R. 030 (14th century); (b) first floor plan with sampling location from R. 139 (14th century) and R. 151 (10th–13th century); (c) third floor plan with sampling location from R. 301 (16th century/1569), R. 302 (16th century/1569) and R. 307 (12th–13th century) (Gerrard 2003).

Figure 3. Ambel preceptory: (a), (b), (c) side view of north-east granary tower, looking west.

Figure 4. Plans and façades of north-east granary tower following the different building phases.

Figure 5. Results from the spatial characteristics survey, including structural discontinuities (cracks) and material discontinuities (variety of construction materials).

Figure 6. PSD analysis. Comparison of local soil sample and rammed earth from R. 307, samples dating to 12th–13th century.

Figure 7. XRD analysis. Comparison of phase data pattern of local soil sample and rammed earth from R. 307, samples dating to 12th–13th century.

Figure 8. XRD analysis. Comparison of phase data pattern of rammed earth from R. 151 (12th century), R. 302 (16th century) and R. 307 (12th–13th century).

Figure 9. MXRF elemental mapping of sample extracted from R. 307. (a) Structure of the material with calcium, silicon and gypsum. The presence of calcium (b), anhydrite or gypsum grains (c) and silicon (d) registers in white.

Figure 10. Moisture content and soluble salts values in historic rammed earth at different wall heights in the east wall of the north-east granary tower.

Figure 11. Compressive strength test carried out on sample material from R. 307 (12th–13th century): (a) extracted sample during test, (b) local soil sample.

Figure 12. Comparison of stress-strain curves between extracted sample and remixed samples.

Figure 13. Location of sensors.

Figure 14. LVDTs used in short-term monitoring (a,b); digital crack meters used medium-term monitoring (c).

Figure 15. Short-term monitoring with LDVTs: crack width variation, inside temperature and RH in different seasons; summer 2011 (a,d), winter 2011 (b,e), summer 2012 (c,f).

Figure 16. Medium-term monitoring with digital crack meters: crack width variation and temperature on east and west façades. A positive sign denotes a crack or interface closing. Sensors M1 and M3 (a), M5 (b), M2 and M4 (c), M6–M7 (d).

Figure 17. Long-term crack monitoring 1997–2012. Sensors L1–L2 and L7 (a); L3–L4 and L8 (b); L5–L6 and L9 (c); L10–L12 (d).

LIST OF TABLES CAPTIONS

Table 1. Results of salt analysis, concentration of cations and anions.

Table 2. Results from compressive strength tests (numbers in brackets are standard deviations).

Table 3. Location of sensors.

Table 4. Results from short-term monitoring 2011–2012.

Table 5. Results from medium-term monitoring 2011–2012.

Figure 1. Ambel preceptory.

108x76mm (300 x 300 DPI)

Figure 2. Ambel preceptory. Location of rammed earth samples: (a) ground floor plan with sampling location from R. 030 (14th century); (b) first floor plan with sampling location from R. 139 (14th century) and R. 151 (10th–13th century); (c) third floor plan with sampling location from R. 301 (16th century/1569), R. 302 (16th century/1569) and R. 307 (12th–13th century) (Gerrard 2003).

219x266mm (300 x 300 DPI)

(a) (b) (c)

Figure 3. Ambel preceptory: (a), (b), (c) side view of north-eastern granary, looking west.

203x83mm (300 x 300 DPI)

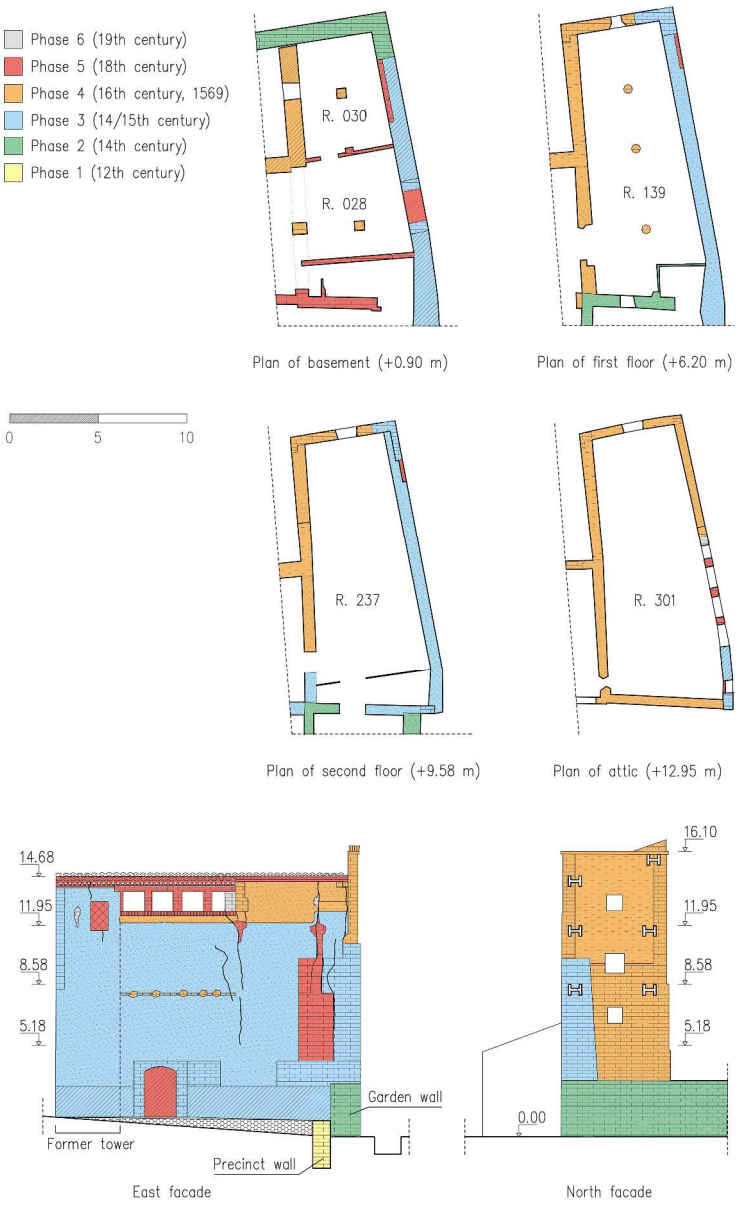

Figure 4. Plans and façades of north-eastern granary tower following the different building phases.

282x459mm (300 x 300 DPI)

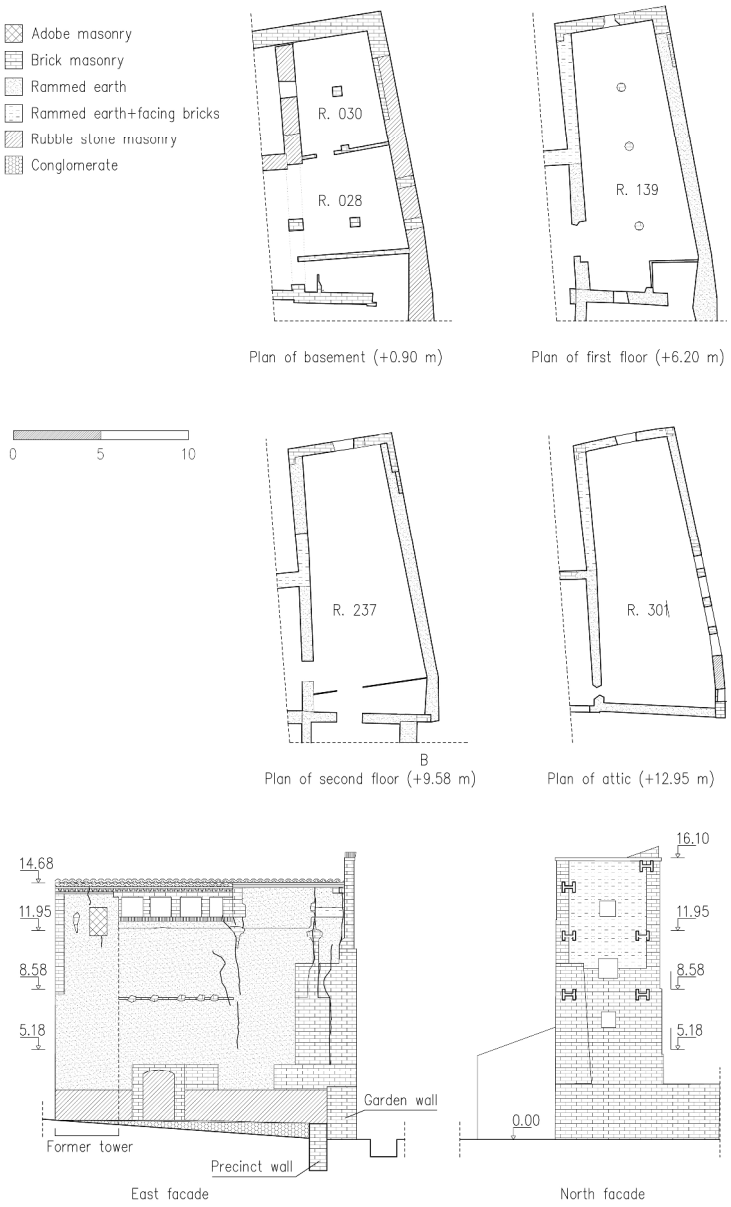

Figure 5. Results from the spatial characteristics survey, including structural discontinuities (cracks) and material discontinuities (variety of construction materials).

281x464mm (300 x 300 DPI)

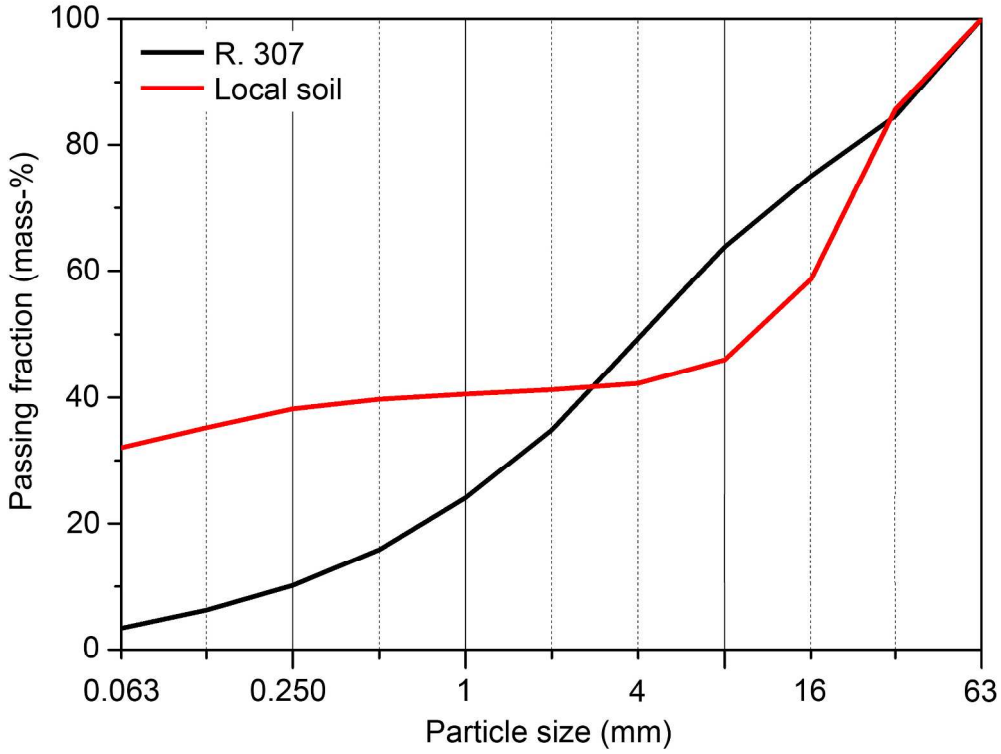

Figure 6. PSD analysis. Comparison of local soil sample and rammed earth from R. 307, samples dating to 12th–13th century.

229x172mm (300 x 300 DPI)

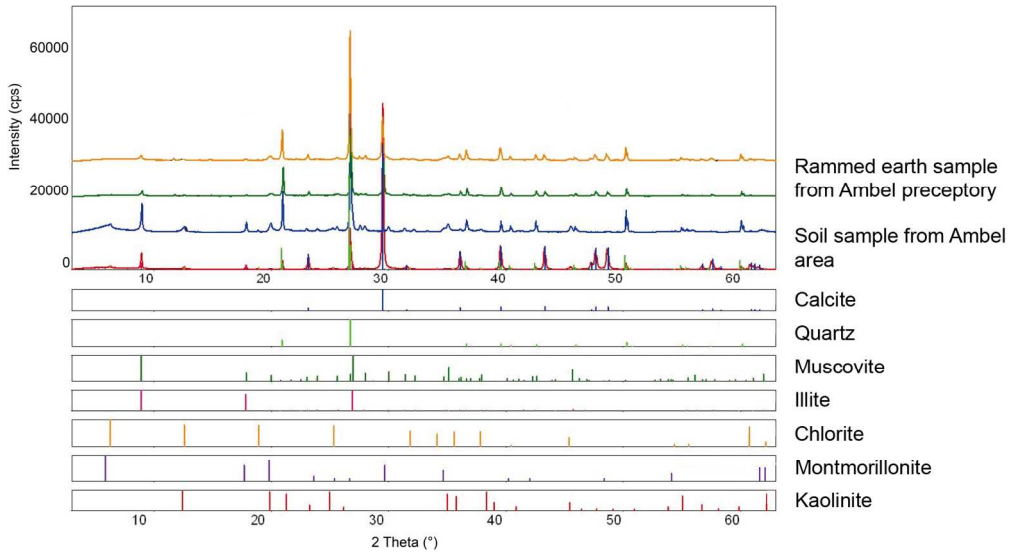

Figure 7. XRD analysis. Comparison of phase data pattern of local soil sample and rammed earth from R. 307, samples dating to 12th–13th century.

157x86mm (300 x 300 DPI)

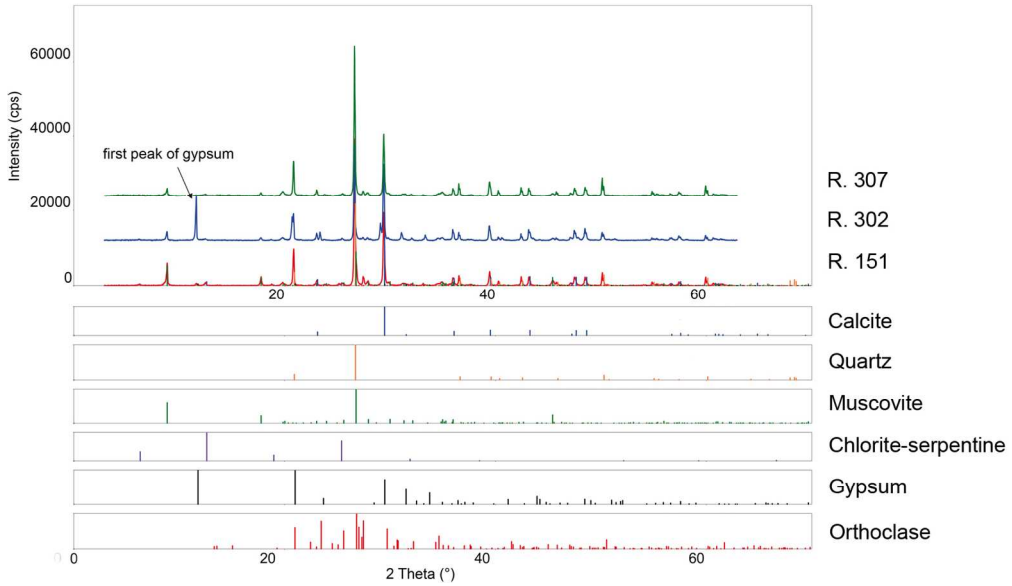

Figure 8. XRD analysis. Comparison of phase data pattern of rammed earth from R. 151 (12th century), R. 302 (16th century) and R. 307 (12th–13th century).

151x87mm (300 x 300 DPI)

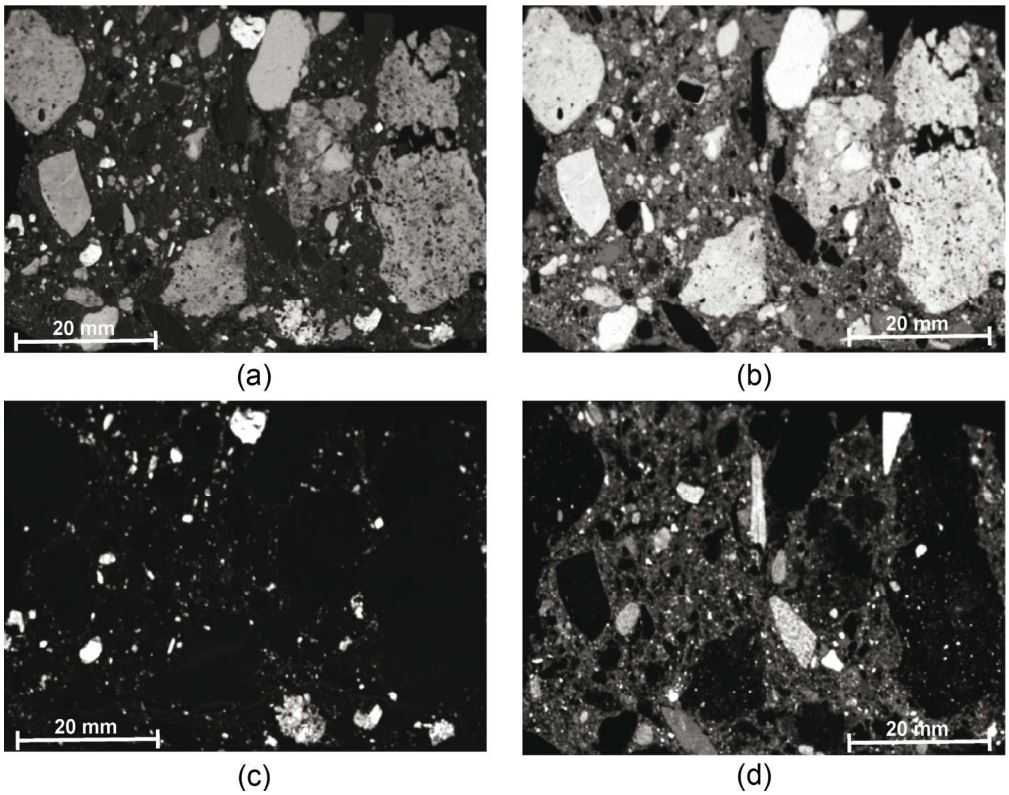

Figure 9. MXRF elemental mapping of sample extracted from R. 307. (a) Structure of the material with calcium, silicon and gypsum. The presence of calcium (b), anhydrite or gypsum grains (c) and silicon (d) registers in white.

170x133mm (300 x 300 DPI)

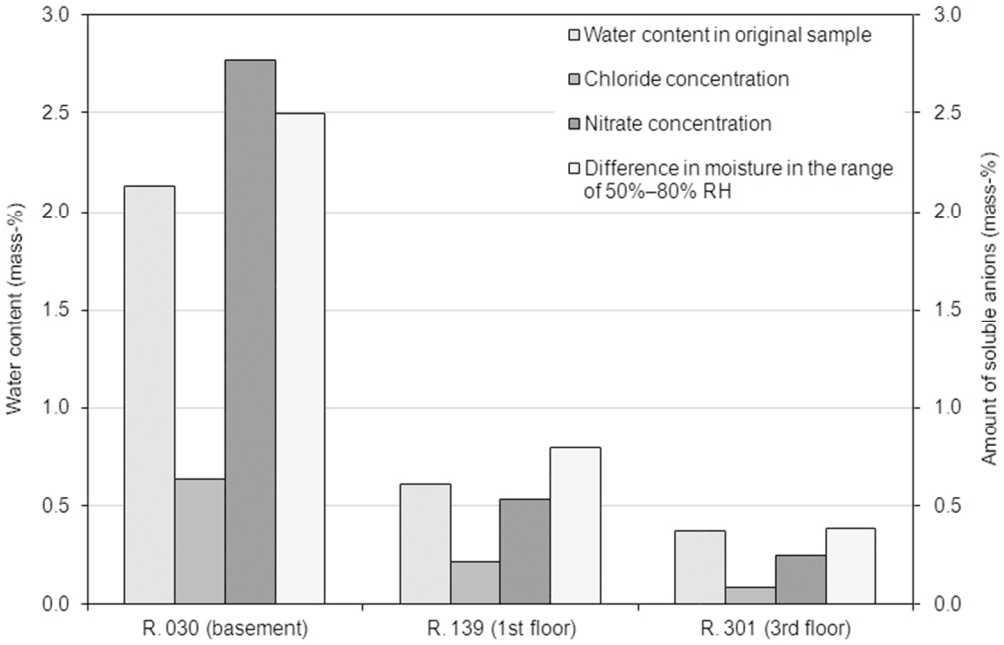

Figure 10. Moisture content and soluble salts values in historic rammed earth at different wall heights in the east wall of the north-east granary tower.

67x42mm (300 x 300 DPI)

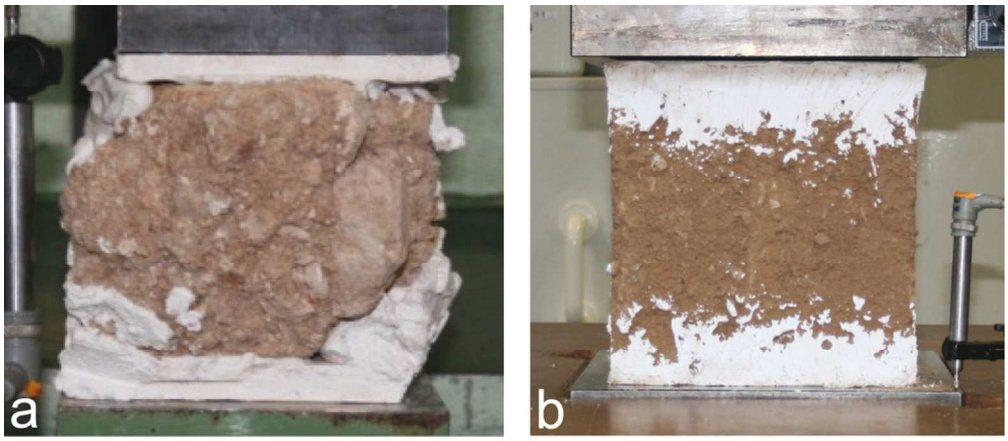

Figure 11. Compressive strength test carried out on sample material from R. 307 (12th–13th century): (a) extracted sample during test, (b) local soil sample.

104x45mm (300 x 300 DPI)

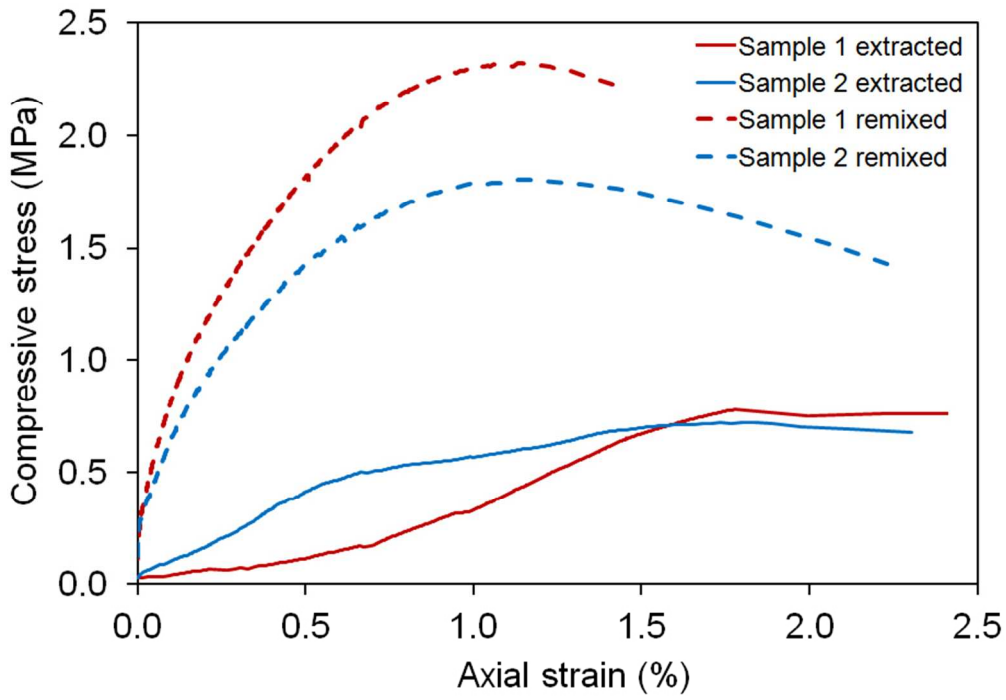

Figure 12. Comparison of stress-strain curves between extracted sample and remixed samples.

77x53mm (300 x 300 DPI)

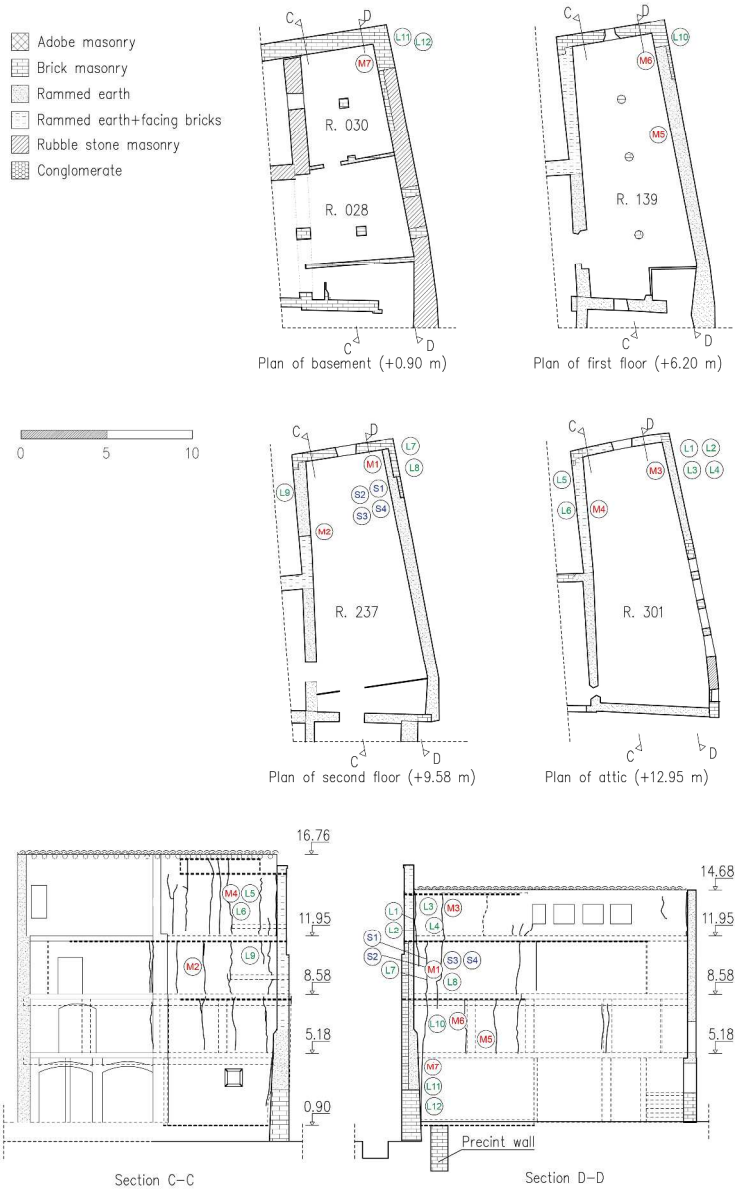

Figure 13. Location of sensors.

280x457mm (300 x 300 DPI)

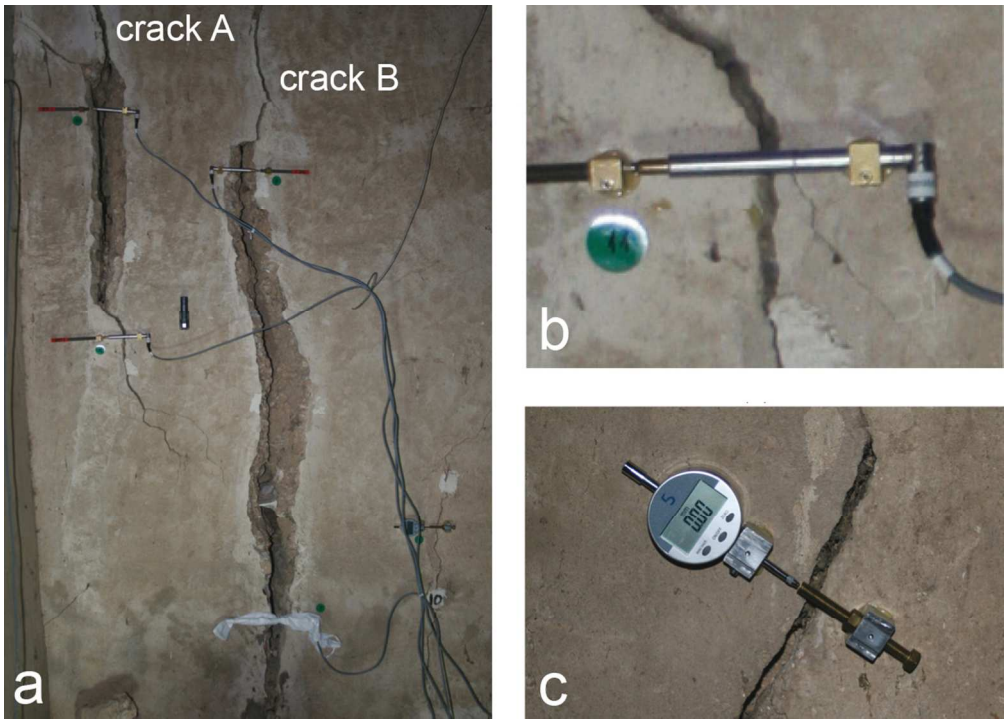

Figure 14. LVDTs used in short-term monitoring (a,b); digital crack meters used medium-term monitoring (c).

106x76mm (300 x 300 DPI)

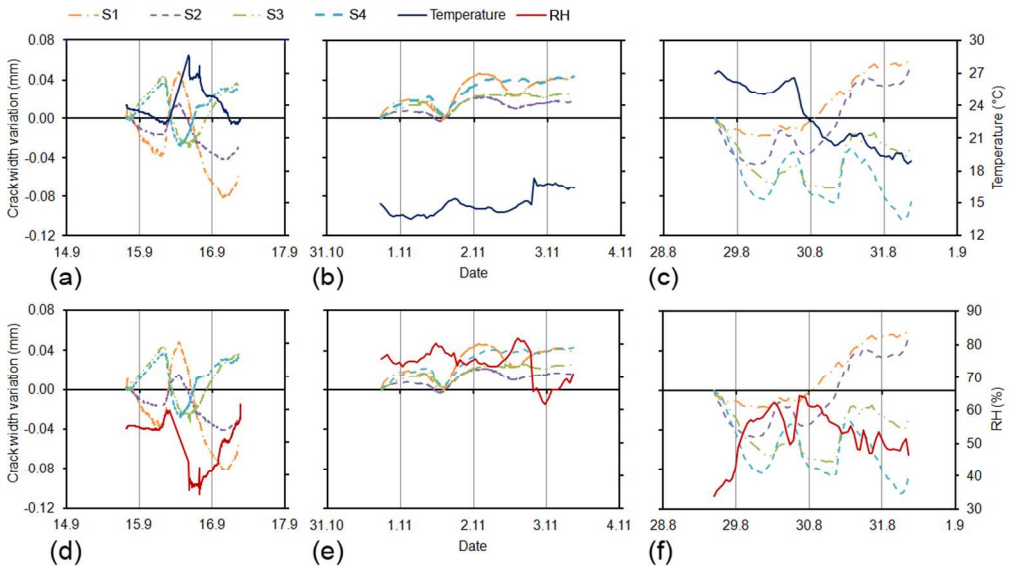

Figure 15. Short-term monitoring with LDVTs: crack width variation, inside temperature and RH in different seasons; summer 2011 (a,d), winter 2011 (b,e), summer 2012 (c,f).

99x56mm (300 x 300 DPI)

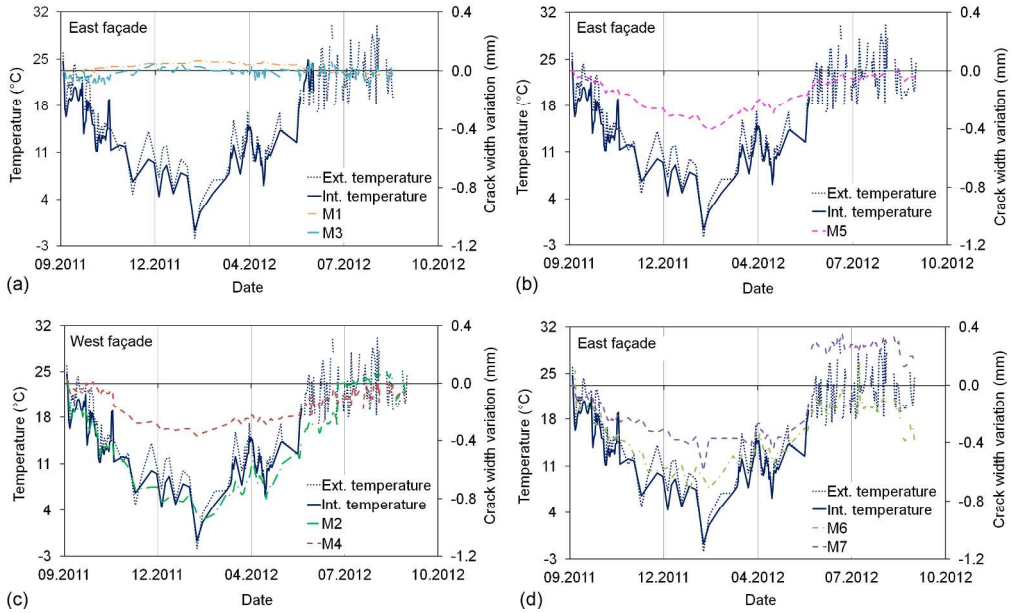

Figure 16. Medium-term monitoring with digital crack meters: crack width variation and temperature on east and west façades. A positive sign denotes a crack or interface closing. Sensors M1 and M3 (a), M5 (b), M2 and M4 (c), M6–M7 (d).

225x136mm (300 x 300 DPI)

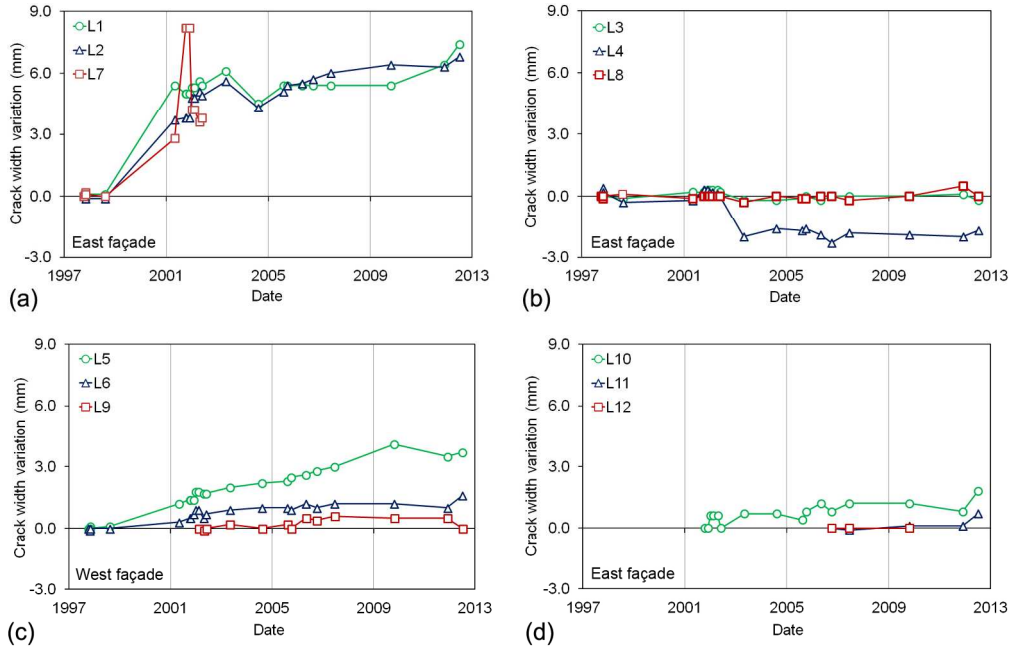

Figure 17. Long-term crack monitoring 1997–2012. Sensors L1–L2 and L7 (a); L3–L4 and L8 (b); L5–L6 and L9 (c); L10–L12 (d).

177x114mm (300 x 300 DPI)

Table 1. Results of salt analysis, concentration of cations and anions.

Room	Height (m)	Comments	Water content (mass-%)	Na^+ (mass-%)	K^+ (mass-%)	Mg^{2+} (mass-%)	Ca^{2+} (mass-%)	Cl^- (mass-%)	NO^{3-} (mass-%)	SO_4^{2-} (mass-%)
R. 030	+3.30	loose, 10 cm cross-sectional reduction	2.13	0.16	0.49	0.09	1.68	0.63	2.77	4.78
	+3.30	loose, 10 cm cross-sectional reduction	2.07	0.16	0.5	0.09	1.69	0.58	2.39	4.55
	+4.30	loose, 2 cm cross-sectional reduction	1.88	0.15	0.39	0.06	1.17	0.42	1.41	2.53
	+4.30	loose, 2 cm cross-sectional reduction	1.96	0.15	0.38	0.06	0.94	0.40	1.49	1.87
R. 139	+5.30	compact	0.61	0.06	0.20	0.05	4.39	0.21	0.53	15.02
	+5.30	compact	0.74	0.07	0.22	0.05	4.00	0.19	0.48	11.58
	+6.30	compact	0.62	0.05	0.17	0.03	3.02	0.20	0.67	10.39
	+6.30	compact	0.53	0.07	0.24	0.04	4.71	0.22	0.78	14.41
	+7.30	compact	0.61	0.10	0.26	0.04	1.38	0.25	0.64	3.63
R. 301	+13.60	reference sample, compact	0.37	0.26	0.12	0.02	2.33	0.08	0.24	6.75

Table 2. Results from compressive strength tests (numbers in brackets are standard deviations).

Rammed earth samples	Bulk density (kg/m^3)	Compressive strength (MPa)	Young's modulus (MPa)	Strain at failure (%)
Extracted	2293 (91)	0.75 (0.04)	56 (36)	1.78 (0.04)
Remixed	2080 (153)	2.07 (0.36)	780 (127)	1.23 (0.04)
Local soil	1960 (33)	1.65 (0.12)	336 (41)	1.01 (0.05)

Table 3. Location of sensors.

Short-term				Long-term			
Sensor	Façade	Floor	Height (m)	Sensor	Façade	Floor	Height (m)
S1	East	2nd	+10.58	L1	East	Attic	+13.95
S2	East	2nd	+9.86	L2	East	Attic	+12.35
S3	East	2nd	+10.42	L3	East	Attic	+13.65
S4	East	2nd	+9.01	L4	East	Attic	+13.15
Medium-term				L5	West	Attic	+13.65
Sensor	Façade	Floor	Height (m)	L6	West	Attic	+13.65
M1	East	2nd	+9.36	L7	East	2nd	+9.86
M2	West	2nd	+10.38	L8	East	2nd	+9.20
M3	East	Attic	+13.95	L9	West	2nd	+11.58
M4	West	Attic	+13.85	L10	East	1st	+6.98
M5	East	1st	+5.71	L11	East	Basement	+3.27
M6	East	1st	+6.98	L12	East	Basement	+2.27
M7	East	Basement	+3.67				

Table 4. Results from short-term monitoring 2011–2012.

Sensor	Crack width variation (mm)				Temperature (°C)	RH (%)
	S1	S2	S3	S4		
September 14th–16th, 2011						
Max value	+0.06	+0.02	+0.03	+0.03	+28.6	59.7
Min value	-0.05	-0.02	-0.05	-0.04	+22.3	34.0
Absolute value	+0.11	+0.05	+0.08	+0.07		
October 31st–November 3rd, 2011						
Max value	+0.03	+0.01	+0.01	+0.02	+17.3	81.7
Min value	-0.02	-0.01	-0.01	-0.01	+13.5	61.7
Absolute value	+0.05	+0.02	+0.02	+0.03		
August 28th–31st, 2012						
Max value	+0.06	+0.05	+0.00	+0.00	+27.2	64.4
Min value	-0.02	-0.05	-0.07	-0.10	+18.7	33.9
Absolute value	+0.08	+0.10	+0.07	+0.10		

Table 5. Results from medium-term monitoring 2011–2012.

Sensor	Crack width variation (mm)							Temperature (°C)	RH (%)
	M1	M2	M3	M4	M5	M6	M7		
October 2011–March 2012									
Max value	+0.02	+0.04	+0.04	+0.07	+0.09	+0.08	+0.22	+22.6	87.6
Min value	-0.06	-0.33	-0.08	-0.28	-0.24	-0.48	-0.27	-2	26.0
Absolute value	+0.08	+0.37	+0.12	+0.35	+0.33	+0.56	+0.49		
April–September 2012									
Max value	+0.02	+0.26	+0.11	+0.09	+0.09	+0.05	+0.65	+29.9	73.5
Min value	-0.03	-0.33	-0.15	-0.28	-0.08	-0.19	-0.27	+6	43.8
Absolute value	+0.05	+0.59	+0.26	+0.37	+0.17	+0.24	+0.92		